

MODELLING DISCRETE MATRIX CRACKS, SPLITS AND CRACK-INDUCED DELAMINATION WITH THE FLOATING NODE METHOD

Bo-Yang Chen*¹, Tong-Earn Tay¹, Silvestre T. Pinho², Vincent B. C. Tan¹

¹Department of Mechanical Engineering, National University of Singapore, EA-07-08, 9 Engineering Drive 1, Singapore

Email(*): boyang.chen.cn@gmail.com

²Department of Aeronautics, Imperial College London. South Kensington Campus, London SW7 2AZ, United Kingdom

Keywords: floating node method, matrix crack, delamination, modelling, failure

Abstract

This paper presents the modelling of matrix cracks, splits and the crack-induced delamination using the floating node method. Enriched ply and cohesive elements are developed to explicitly represent the matrix cracks in plies and the crack boundaries on the interfaces. A laminate element is formed, such that a fixed, planar mesh can be used for laminates of arbitrary layups. The application examples demonstrate that the proposed method is capable of predicting several challenging scenarios of composites failure, such as the large number matrix cracks, grip-to-grip longitudinal splits, widespread delamination, etc.

1. Introduction

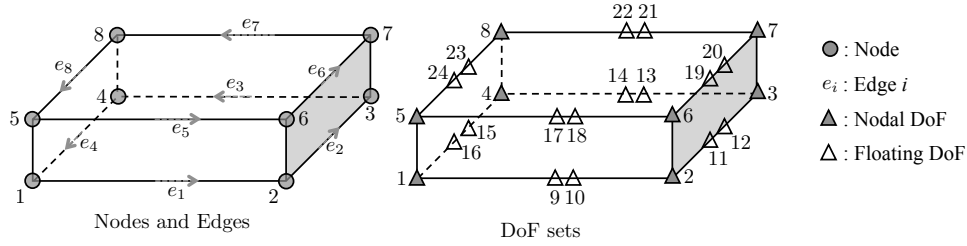
The progressive failure of composites often involves the development of a large quantity of matrix cracks and delamination [1, 2]. The blocking of the 0 plies promotes the development of longitudinal matrix splits, sometimes from grip to grip. They cause widespread delamination, which subsequently lead to the disintegration of the laminate prior to the breaking of the 0 ply-block [1, 2]. This paper presents a three-dimensional (3D), composites-oriented development of the Floating Node Method (FNM) [3, 4], demonstrated on the modelling of matrix cracks, longitudinal splits and delamination in ply-blocked laminates.

2. Theory

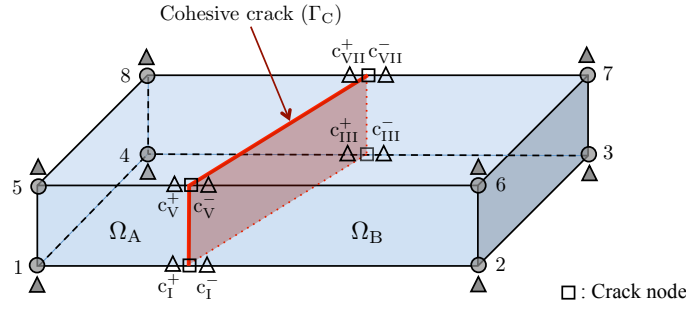
In the FNM, the definition of an element is enriched to include both node connectivity and edge connectivity. In addition to allocating DoFs to the nodes, DoFs are also allocated to the edges. In contrast to the nodal DoFs, the DoFs of edges are called *floating* DoFs. Floating DoFs can be freely allocated to any geometrical entity, and be used to represent the DoF of an arbitrary node on this entity, the location of which may not be known a priori [3, 4].

2.1. Enriched ply element

An enriched ply element can be constructed with the FNM, such that a matrix crack can be modelled within its domain. Figure 1a shows the node, edge and DoF definitions of this element. It is assumed that only the horizontal edges are crossed by the matrix crack. This is applicable when the matrix crack is



(a) The definitions of an enriched ply element.



(b) A matrix crack introduces four pairs of coinciding crack nodes on four edges of the element.

Figure 1: An enriched ply element by FNM.

perpendicular to the shell plane, which is typically the case in in-plane loading situations. Floating DoF sets are only allocated to the horizontal edges Figure 1a. Before matrix cracking, the static equilibrium of a body with volume Ω under body forces with density \mathbf{f} (acting on Ω) and traction \mathbf{t} acting on the boundary Γ_t can be expressed in the weak form as:

$$\int_{\Omega} \boldsymbol{\epsilon}^T(\mathbf{v}) \boldsymbol{\sigma}(\mathbf{u}) \, d\Omega = \int_{\Omega} \mathbf{v}^T \mathbf{f} \, d\Omega + \int_{\Gamma_t} \mathbf{v}^T \mathbf{t} \, d\Gamma \quad (1)$$

where \mathbf{u} is the displacement solution, \mathbf{v} is the test function, $\boldsymbol{\epsilon}$ is the strain tensor (related to \mathbf{u} through the differential operator relative to Cartesian coordinates $\mathcal{L}_{\mathbf{x}}$ as $\boldsymbol{\epsilon} = \mathcal{L}_{\mathbf{x}}(\mathbf{u})$), and $\boldsymbol{\sigma}$ is the stress tensor (related to the strains through Hook's law as $\boldsymbol{\sigma} = \mathbf{D}\boldsymbol{\epsilon}$, with \mathbf{D} being the constitutive tensor). In this case, the ply element is a standard linear brick element. The crack nodes do not exist, and the floating DoFs are not used.

When a certain failure criterion or propagation criterion is met, a matrix crack initiates or propagates within the element domain. Assuming that the matrix crack is a cohesive crack, the weak form of the equilibrium equation now becomes:

$$\int_{\Omega_A \cup \Omega_B} \boldsymbol{\epsilon}^T(\mathbf{v}) \boldsymbol{\sigma}(\mathbf{u}) \, d\Omega + \int_{\Gamma_C} [[\mathbf{v}]]^T \boldsymbol{\tau}_c([[\mathbf{u}]]) \, d\Gamma = \int_{\Omega_A \cup \Omega_B} \mathbf{v}^T \mathbf{f} \, d\Omega + \int_{\Gamma_t} \mathbf{v}^T \mathbf{t} \, d\Gamma \quad (2)$$

where $[[\bullet]]$ represents the jump of a function between the top and bottom surfaces of the cohesive crack, and $\boldsymbol{\tau}_c$ is the traction acting between the surfaces of the cohesive crack. $\boldsymbol{\tau}_c$ relates to the separation of the top and bottom surfaces of the cohesive crack, $[[\mathbf{u}]]$, through a constitutive relationship of the form:

$$\boldsymbol{\tau}_c = \mathbf{D}_{CE} [[\mathbf{u}]] \quad (3)$$

where \mathbf{D}_{CE} is the cohesive constitutive tensor.

Supposing that the matrix crack cuts across four edges of the element, for instance, e_1 , e_3 , e_5 and e_7 , then it creates four pairs of initially coinciding crack nodes, c_1^{\pm} , c_{III}^{\pm} , c_V^{\pm} and c_{VII}^{\pm} , on the four edges,

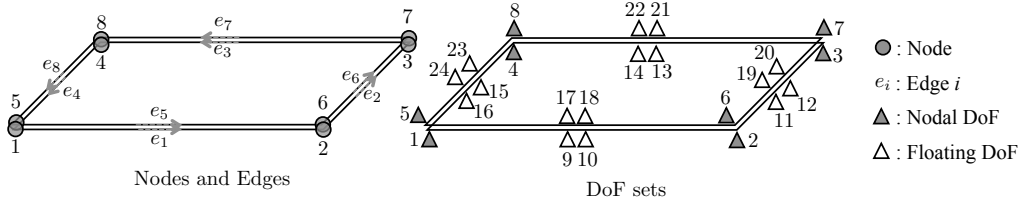


Figure 2: The definitions of an enriched cohesive element.

respectively (Figure 1b). The coordinates of the crack nodes are the intersections of the crack and the edges. The matrix crack partitions the original domain Ω into two subdomains, Ω_A and Ω_B , with Γ_C being the crack interface. Three Sub-Elements (SEs) can be formed, such that they represent the two bulk subdomains Ω_A and Ω_B and the cohesive crack Γ_C . Note that the nodal coordinates of these SEs are fully defined by the original nodes and crack nodes. With the floating DoF sets allocated to the cracked edges, the DoF vectors (i.e., \mathbf{u}_{Ω_A} , \mathbf{u}_{Ω_B} , \mathbf{u}_{Γ_C}) of the three SEs are also fully defined. Under the assumption of isoparametric representation, the displacement solution is:

$$\begin{aligned} \mathbf{u}(\mathbf{x}) &= \mathbf{N}_{\Omega_A}(\mathbf{x}) \mathbf{u}_{\Omega_A}, \text{ if } \mathbf{x} \in \Omega_A; \\ &= \mathbf{N}_{\Omega_B}(\mathbf{x}) \mathbf{u}_{\Omega_B}, \text{ if } \mathbf{x} \in \Omega_B, \end{aligned} \quad (4)$$

with

$$[[\mathbf{u}]](\mathbf{x}) = \mathbf{N}_{\Gamma_C}(\mathbf{x}) \mathbf{u}_{\Gamma_C}, \text{ if } \mathbf{x} \in \Gamma_C, \quad (5)$$

where \mathbf{N}_{Ω_A} , \mathbf{N}_{Ω_B} and \mathbf{N}_{Γ_C} are the standard finite element shape function matrices (in physical coordinates) of the elements defined by Ω_A , Ω_B and Γ_C , respectively. The stiffness matrices (i.e., \mathbf{K}_{Ω_A} , \mathbf{K}_{Ω_B} , \mathbf{K}_{Γ_C}) and force vectors (i.e., \mathbf{Q}_{Ω_A} , \mathbf{Q}_{Ω_B} , \mathbf{Q}_{Γ_C}) of the SEs can be calculated using standard finite element integration techniques. The weak form of the equilibrium equation, Equation (2), can be written in an assembled form as:

$$\mathbf{K}_{el} \mathbf{u}_{el} = \mathbf{Q}_{el} \quad (6)$$

with:

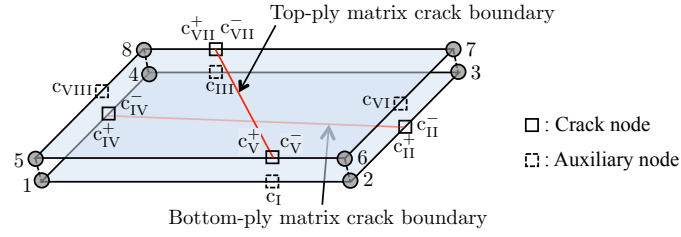
$$\begin{aligned} \mathbf{K}_{el} &= \mathcal{A}(\mathbf{K}_{\Omega_A}, \mathbf{K}_{\Omega_B}, \mathbf{K}_{\Gamma_C}), \\ \mathbf{u}_{el} &= \mathcal{A}(\mathbf{u}_{\Omega_A}, \mathbf{u}_{\Omega_B}, \mathbf{u}_{\Gamma_C}), \\ \mathbf{Q}_{el} &= \mathcal{A}(\mathbf{Q}_{\Omega_A}, \mathbf{Q}_{\Omega_B}, \mathbf{Q}_{\Gamma_C}), \end{aligned} \quad (7)$$

where \mathcal{A} is the assembly operator.

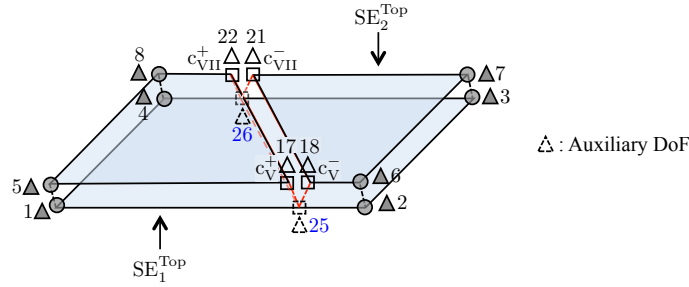
2.2. Enriched cohesive element

Previous studies have shown that the explicit modelling of matrix crack boundaries on the interfaces is necessary to accurately predict the matrix crack/delamination interaction [3, 5]. In 3D laminates, matrix cracks may occur on both sides of the interface. In order to capture the stress concentrations induced by both matrix cracks, an enriched cohesive element is formulated. It consists of two initially coinciding surfaces, defined by both its nodes and its edges. A pair of floating DoF sets are allocated to each edge of the element (Figure 2). Before any matrix crack appearing from the top or bottom ply element, the cohesive element is a standard 8-node linear cohesive element.

If a matrix crack occurs on the top ply element and, for instance, cuts across edges e_5 and e_7 on the top surface of the cohesive element (Figure 3a), then it creates two pairs of initially coinciding crack nodes on these edges, i.e., c_{VI}^+ and c_{VII}^+ , respectively. Two auxiliary nodes which initially coincide with the crack nodes can be located on the bottom surface of the cohesive element, i.e., c_I and c_{III} . These nodes allow the



(a) Matrix cracks from top and bottom plies may cut across four edges of the element.



(b) SE^{Top} and its SEs, SE_1^{Top} and SE_2^{Top} , with respect to the matrix crack boundary on the top surface.

Figure 3: An enriched cohesive element by the FNM.

nodal coordinates of the two SEs, namely SE_1^{Top} and SE_2^{Top} (see Figure 3b), to be defined. With the use of the floating DoFs, the DoF vectors (i.e., $\mathbf{u}_{SE_1^{Top}}$, $\mathbf{u}_{SE_2^{Top}}$) of the two SEs can be formed. The separation at location \mathbf{x} , $[[\mathbf{u}]](\mathbf{x})$, is:

$$\begin{aligned} [[\mathbf{u}]](\mathbf{x}) &= \mathbf{N}_{SE_1^{Top}}(\mathbf{x}) \mathbf{u}_{SE_1^{Top}}, \text{ if } \mathbf{x} \in \Omega_{SE_1^{Top}}, \\ [[\mathbf{u}]](\mathbf{x}) &= \mathbf{N}_{SE_2^{Top}}(\mathbf{x}) \mathbf{u}_{SE_2^{Top}}, \text{ if } \mathbf{x} \in \Omega_{SE_2^{Top}}, \end{aligned} \quad (8)$$

where $\mathbf{N}_{SE_1^{Top}}$ and $\mathbf{N}_{SE_2^{Top}}$ are shape function matrices (in physical coordinates) of the cohesive SEs on SE_1^{Top} and SE_2^{Top} , respectively. The stiffness matrices of the two SEs, $\mathbf{K}_{SE_1^{Top}}$ and $\mathbf{K}_{SE_2^{Top}}$, can be calculated using the procedure detailed in [6]. The stiffness matrix of SE^{Top} in Figure 3b is obtained from the assembly of those of the two SEs:

$$\mathbf{K}_{SE^{Top}} = \mathcal{A} \left(\mathbf{K}_{SE_1^{Top}}, \mathbf{K}_{SE_2^{Top}} \right). \quad (9)$$

Similarly, if a matrix crack occurs on the bottom ply element, the element (here named SE^{Bot}) can be partitioned and integrated using the same procedure as that of SE^{Top} . If both the top and bottom matrix cracks are present, then both SE^{Top} and SE^{Bot} are integrated. Their integrations are performed over the same domain, i.e., the domain of the whole cohesive element. In this case, it is assumed that the solution is a superposition of those of the two SEs, each carrying half of the weight. The final stiffness matrix of the whole cohesive element is therefore the weighted superposition of those of SE^{Top} and SE^{Bot} :

$$\mathbf{K}_{CE} = \mathcal{A} \left(\frac{1}{2} \mathbf{K}_{SE^{Top}}, \frac{1}{2} \mathbf{K}_{SE^{Bot}} \right) \quad (10)$$

2.3. A laminate element

With the enriched ply and cohesive elements defined in the previous sections, a laminate element can be formed, such that ply and cohesive elements are SEs of the laminate element (Figure 4). Note that all

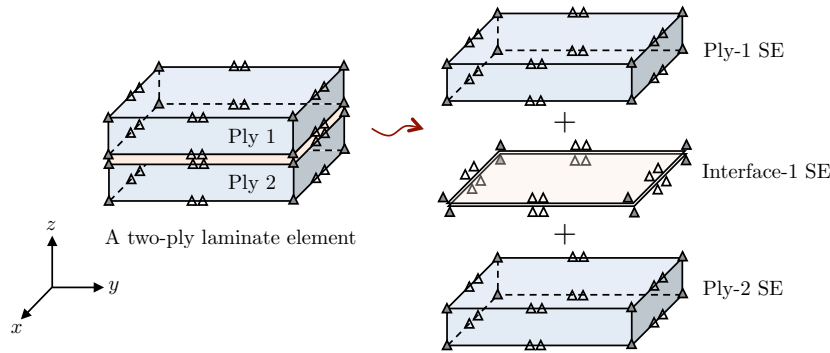


Figure 4: A laminate element can be constructed based on layup

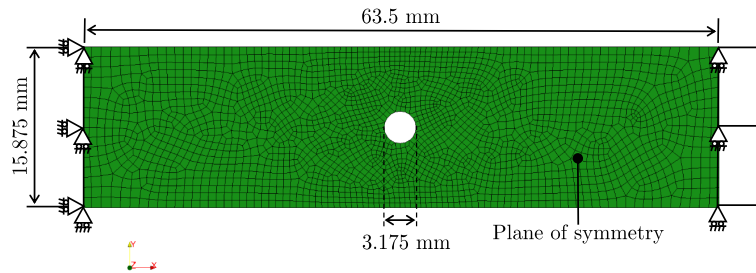


Figure 5: Finite element model of OHT laminate under tension.

the SEs are within the same laminate element, facilitating the exchange of information between different SEs. In addition, the use of such a laminate element greatly reduces the effort of preprocessing. The layup and ply thickness are defining parameters of this element, and they do not need to be reflected in the mesh.

2.4. Crack propagation

With the edge connectivity available for each element, an edge status variable approach is developed for the modelling of cohesive crack propagations in FNM. A list of all the edges is created, where a status variable, μ , and a coordinates vector, \mathbf{x}_c , are allocated to every edge. μ stores the current status of the edge, i.e., intact, hosting a crack tip, or already at the wake of the crack tip. \mathbf{x}_c stores the coordinates of the crack node on the edge. An element only needs to read a fixed amount of information to propagate a crack, i.e., the edge status variables of its own edges, regardless of the total number of cracks in the mesh.

3. Applications

The elements presented in the previous sections are implemented as user-defined elements in the commercial finite element package Abaqus, and are applied on the modelling of the tensile failure of notched and unnotched $[45_4/90_4/-45_4/0_4]_s$ IM7/8552 carbon/epoxy laminates [1, 2]. All analysis in this section are quasi-static, performed using the implicit method.

3.1. Tensile failure of notched $[45_4/90_4/-45_4/0_4]_s$ laminate

The progressive tensile failure of the Open-Hole Tension (OHT) of $[45_4/90_4/-45_4/0_4]_s$ laminate in [1] is modelled in this section. The experimental image shows that the laminate has disintegrated at final failure, where the delamination has completely separated the angle plies with the 0 plies. The finite

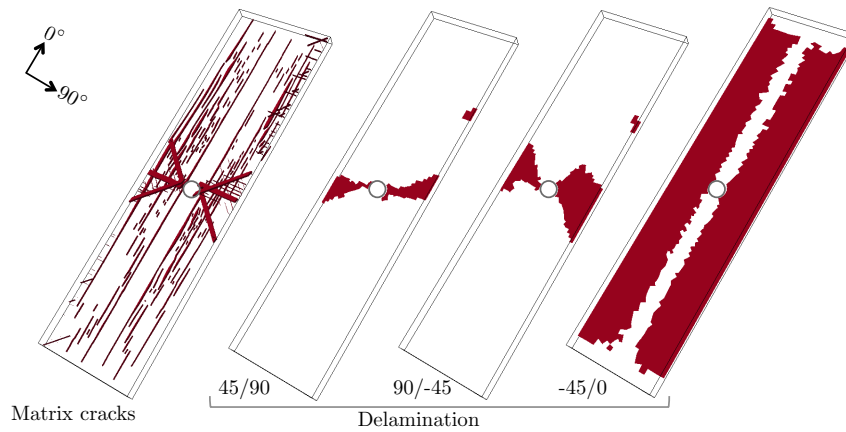


Figure 6: Failure pattern predictions of the OHT $[45_4/90_4/ - 45_4/0_4]_s$ laminate in [1].

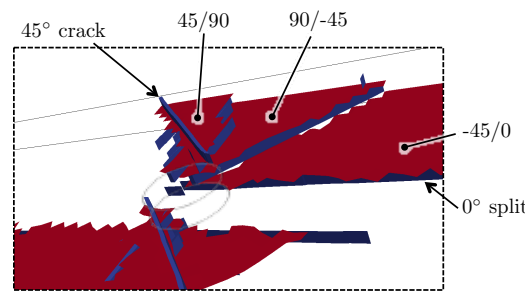


Figure 7: The “staircase” delamination patterns.

element model is shown in Figure 5. Only half of the laminate is considered, with the symmetric boundary condition applied on the laminate midplane. The transverse displacement is constrained at the grip ends to approximate the effect of gripping. Note that a planar mesh is used, no meshing in the thickness direction is needed. A randomly-generated, unstructured mesh is purposely used to demonstrate the effectiveness of the FNM on arbitrary meshes. Each element is a laminate element with 4 ply-blocks and 3 interfaces, defined based on the layup (ref. Section 2.3). The elements are about $0.5 \text{ mm} \times 0.5 \text{ mm}$ in dimension in the region around the hole, and $1 \text{ mm} \times 1 \text{ mm}$ in the regions away from the hole. The predicted strength of the laminate is 295 MPa, which agrees well with the experimental average of 275 MPa [1]. The simulated damage patterns at failure are summarized in Figure 6. The red area shows cohesive elements which have reached total failure. Prior to failure, a “staircase” delamination pattern can be observed as shown in Figure 7, where delamination follows the boundaries set by the matrix cracks. A close agreement is reached between the predicted patterns and the experimental observations in [1].

3.2. Tensile failure of unnotched $[45_4/90_4/ - 45_4/0_4]_s$ laminate

The progressive tensile failure of the unnotched $[45_4/90_4/ - 45_4/0_4]_s$ laminate in [2] is simulated in this section. Similarly to the previous case, the experimental observations in [2] show that the laminate has disintegrated at final failure, where the delamination has completely separated the angle plies with the 0 plies. It is also reported that the failure of 0 plies initiates from the grip, accompanied by the development of extensive longitudinal splits. The finite element model is the same as that of the previous case, except that no hole is present in the specimen. A structured mesh is used, with elements being about $1 \text{ mm} \times 1 \text{ mm}$ in dimension. The predicted strength of the laminate is 526 MPa, which agrees well with the experimental average of 541 MPa [2]. Prior to final failure, the out-of-plane displacement contour prediction in Figure 8 clearly shows the peel-off of both the 45 and the 90 plies. The simulated

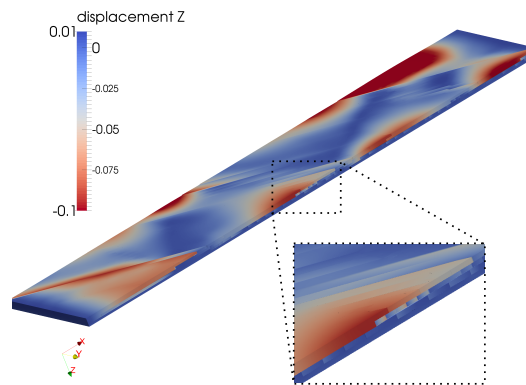


Figure 8: The predicted out-of-plane displacement contour shows the peel-off of the 45° and 90° plies from the edge.

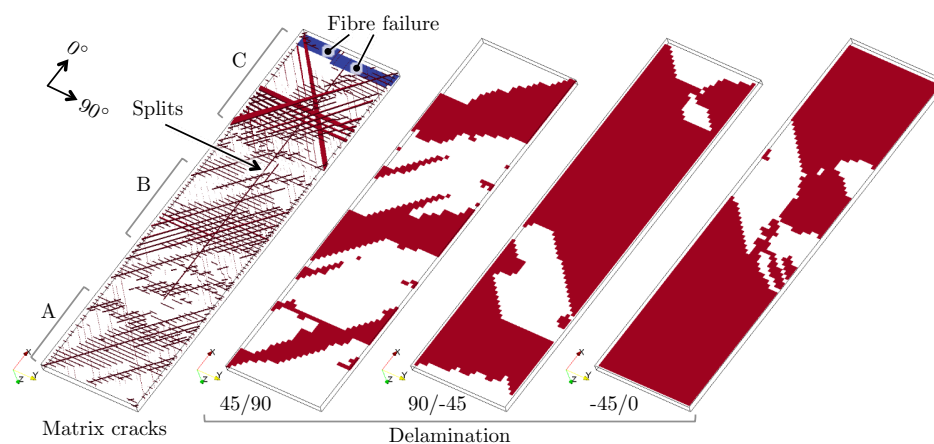


Figure 9: Failure pattern predictions of the unnotched $[45_4/90_4/-45_4/0_4]_s$ laminate in [2].

damage patterns at final failure are presented in Figure 9. The red area shows cohesive elements which have reached total failure. Three zones with a high concentration of matrix cracks can be identified in the predicted matrix crack patterns (marked with A, B and C in Figure 9). The final failure of the laminate is marked with the sudden appearance of fibre failure in the grip region in Zone C and a longitudinal split which spans across more than 2/3 of the length of the laminate. The widespread delamination on the 90/-45 and -45/0 interfaces, together with the opened cracks in Zone C, indicate that the laminate has disintegrated.

4. Conclusion

This paper presents the high-fidelity modelling of matrix cracks, splits, and crack-induced delamination in composites. A three-dimensional (3D), composites-oriented Floating Node Method (FNM) is developed. The 3D FNM is applied on the modelling of the progressive tensile failure of ply-blocked, quasi-isotropic laminates. It is shown that the proposed method accurately predicts the extent of matrix cracks and splits, the thereby induced delamination, and the subsequent widespread propagation of the delamination which causes the disintegration of the laminate.

Acknowledgments

The authors would like to acknowledge the research grant (No. R265000463112) from the Ministry of Education of Singapore, and the strategic funding (No. R265000523646) from National University of Singapore.

References

- [1] B. G. Green, M. R. Wisnom, and S. R. Hallett. An experimental investigation into the tensile strength scaling of notched composites. *Composites Part A-Applied Science and Manufacturing*, 38(3):867–878, 2007.
- [2] M. R. Wisnom, B. Khan, and S. R. Hallett. Size effects in unnotched tensile strength of unidirectional and quasi-isotropic carbon/epoxy composites. *Composite Structures*, 84(1):21–28, 2008.
- [3] B. Y. Chen, S. T. Pinho, N. V. De Carvalho, P. M. Baiz, and T. E. Tay. A floating node method for the modelling of discontinuities in composites. *Engineering Fracture Mechanics*, 127:104 – 134, 2014.
- [4] N. V. De Carvalho, B. Y. Chen, S. T. Pinho, J. G. Ratcliffe, P. M. Baiz, and T. E. Tay. Modeling delamination migration in cross-ply tape laminates. *Composites Part A: Applied Science and Manufacturing*, 71:192–203, 2015.
- [5] X. J. Fang, Q. D. Yang, B. N. Cox, and Z. Q. Zhou. An augmented cohesive zone element for arbitrary crack coalescence and bifurcation in heterogeneous materials. *International Journal for Numerical Methods in Engineering*, 88:841–861, 2011.
- [6] P. P. Camanho, C. G. Dávila, and M. F. de Moura. Numerical simulation of mixed-mode progressive delamination in composite materials. *Journal of Composite Materials*, 37(16):1415–1438, 2003.